

Supporting Information

**A Membrane-Free Redox Flow Battery with Two Immiscible Redox Electrolytes**

*Paula Navalpotro, Jesus Palma, Marc Anderson, and Rebeca Marcilla\**

anie\_201704318\_sm\_miscellaneous\_information.pdf

## **Author Contributions**

R.M. Conceptualization: Lead; Funding acquisition: Lead; Investigation: Equal; Methodology: Equal; Project administration: Lead; Resources: Lead; Supervision: Lead; Validation: Lead; Visualization: Lead; Writing—original draft: Equal; Writing—review & editing: Lead

p.n. Formal analysis: Lead; Investigation: Equal; Methodology: Equal; Writing—original draft: Equal

m.a. Validation: Supporting; Visualization: Supporting; Writing—original draft: Supporting

j.p. Supervision: Supporting; Validation: Supporting; Visualization: Supporting; Writing—original draft: Supporting.

## Table of content

Materials and Methods	1
Table S1: Comparison of technical parameters and key factors of reported Organic-RFBs	4
Figure S1. Electrochemical investigation of redox electrolytes using a Rotating Disk Electrode (RDE)	5
Figure S2. Polarization curves of our Membrane-Free battery at four different states of charge (SOC).	6
Figure S3. Cyclability test of our Membrane-Free battery at profound depth of discharge (DoD) from 35 % to 0 % SOC	7
Figure S4. Membrane-Free battery performance at higher concentration of active species (0.1 M pBQ in PYR <sub>14</sub> TFSI and 0.1 M H <sub>2</sub> Q in 0.1 M HCl)	8
Figure S5. Elucidation of effect of crossover of active species through the interphase on battery performance. Electrochemical investigation of the two immiscible electrolytes before and after cycling.	9
References	10

## Materials and Methods

### Materials.

N-butyl-N-methylpyrrolidinium bis(trifluoromethanesulfonyl) imide (PYR<sub>14</sub>TFSI) having a 99.5% purity was purchased from Solvionic. p-Benzoquinone (pBQ) (> 99.5% purity) was obtained from Fluka Analytical and Hydroquinone (H<sub>2</sub>Q) reagent (> 99% purity) was purchased from Sigma Aldrich and used as received for electrolyte preparation. Hydrochloric acid (37 %) laboratory reagent grade was purchased from Fischer Chemical and used as received.

### Preparation of Electrolytes.

The positive electrolyte or catholyte was prepared by dissolving H<sub>2</sub>Q (22 mg) in ultrapure water (10 ml) and by adding a 37% HCl solution (83 μl) to afford a 20 mM H<sub>2</sub>Q in 0.1 M HCl. The negative electrolyte or anolyte was prepared by dissolving pBQ (21.6 mg) in PYR<sub>14</sub>TFSI (10 ml) to obtain a solution 20 mM of pBQ in PYR<sub>14</sub>TFSI. The same method was used to produce the highly concentrated redox electrolytes; 0.1 M H<sub>2</sub>Q in 0.1 M HCl and 0.1 M pBQ in PYR<sub>14</sub>TFSI. For RDE experiments, 5.4 mg of pBQ were dissolved in PYR<sub>14</sub>TFSI (10 ml) in order to afford a more diluted solution 5 mM pBQ in PYR<sub>14</sub>TFSI. Preparation of ionic liquid electrolytes was performed inside a MBraun glove box (O<sub>2</sub> and H<sub>2</sub>O < 0.1 ppm).

### Electrode pretreatment.

Permeable carbon felts provided by SGL CARBON GmbH (grade GFD4.6 EA) (4.6 mm thickness) were cut into squared coupons (geometric surface area ~5 cm<sup>2</sup>) and used as electrode material in our Membrane-Free batteries. The electrodes were pretreated by immersion in 1 M NaOH solution at 80°C during 1 h. After washing with ultrapure water, they were dried at 100°C overnight.

### Electrochemical characterization or redox electrolytes.

All electrochemical tests were conducted using a Biologic VMP multichannel potentiostat. A glassy carbon electrode (ID: 3 mm) and a platinum mesh were used as working and counter-electrodes respectively for three-electrode cyclic voltammetry (CV) tests. Ag/AgCl was used as reference electrode in the aqueous electrolyte and a Ag wire was used as pseudo-reference electrode in the ionic liquid electrolyte.

Rotating-disk electrode (RDE) experiments were performed using a BASi RDE-2 rotating-disk electrode system (Supplementary Fig.1). All tests were obtained using a three-electrode cell with a glassy carbon rotating electrode (ALS Co., Ltd). Counter and reference electrodes were the same as those for the three-electrode CV test. Linear sweep voltammetry (LSV) measurements were conducted at a scan rate of 10 mVs<sup>-1</sup> over a range of rotation rates (400 rpm to 3000 rpm). Before and during testing, the electrolytes were purged with ultra-high purity Argon to ensure adequate deaeration. Diffusion coefficients (*D*) and heterogeneous rate constants (*K*<sup>0</sup>) were calculated using the Koutecky- Levich equation (Eq.1).

$$\frac{1}{i} = \frac{1}{i_K} + \frac{1}{i_l} \quad (1)$$

$$\text{Where: } i_l = 0.62 n F A D^{2/3} \omega^{1/2} \vartheta^{-1/6} C; \quad \text{and} \quad i_K = nFAK^0C$$

and  $n$  is the number of electrons transferred,  $F$  the Faraday constant,  $A$  the disc area,  $D$  the diffusion coefficient,  $\vartheta$  the kinematic viscosity,  $C$  the electroactive species concentration and  $K^0$  the heterogeneous rate constant. A Levich plot was constructed from the RDE data by plotting the mass-transport limited current vs. the square root of the rotation rate (Supplementary Figs 1b and 1d).

The diffusion coefficient calculated for H<sub>2</sub>Q in 0.1 M HCl was  $4.1 \cdot 10^{-4} \text{ cm}^2\text{s}^{-1}$ , which was higher than for the same molecule in sulfuric acid ( $D \sim 10^{-6} \text{ cm}^2\text{s}^{-1}$ ) [1], organic ( $D \sim 10^{-5} - 10^{-6} \text{ cm}^2\text{s}^{-1}$ ) [2,3] or neutral electrolytes ( $D = 10^{-4} - 10^{-5} \text{ cm}^2\text{s}^{-1}$ ) [4,5]. Moreover, the fast kinetics of H<sub>2</sub>Q was corroborated with the high rate constant ( $K^0 = 0.379 \text{ cms}^{-1}$ ) that is in the same range of recent published results [6]. For the ionic liquid redox electrolyte, two diffusion coefficients ( $D$ ), for pBQ and pBQ<sup>•</sup>, were found to be  $5.8 \cdot 10^{-5} \text{ cm}^2\text{s}^{-1}$  and  $8.64 \cdot 10^{-5} \text{ cm}^2\text{s}^{-1}$ , respectively. The resulting rate constants ( $K^0$ ) were  $1.2 \cdot 10^{-3} \text{ cms}^{-1}$  for pBQ → pBQ<sup>•</sup> and  $7.72 \cdot 10^{-3} \text{ cms}^{-1}$  for pBQ<sup>•</sup> → pBQ<sup>2-</sup>. Those values are similar to those reported by other groups in aprotic electrolytes [7-9].

### **Battery Assembly.**

Due to the immiscibility of the two electrolytes, a biphasic liquid-liquid system was formed spontaneously when 4 ml of the aqueous electrolyte (catholyte) was mixed with 4 ml of IL electrolyte (anolyte) in a cylindrical electrochemical cell of 2.5 cm diameter. The aqueous electrolyte occupied the upper phase and the ionic liquid electrolyte formed the lower phase of this system. One carbon felt electrode (squared shape of 5 cm<sup>2</sup>) was immersed in each phase forming the positive and negative terminals. The distance between two carbon electrodes was approximately 2 cm. No ion-exchange membrane or physical separator was used to separate the two redox electrolytes. As such, they are genuinely separated by the “natural” interphase. In order to follow the voltage evolution of the individual electrolyte and the voltage difference through the interphase, two reference electrodes were immersed into each electrolyte; Ag/AgCl in the aqueous phase and the silver wire in the ionic liquid phase. For all full cell studies, electrolytes were assembled in a fully discharged state.

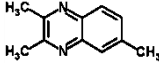
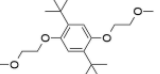
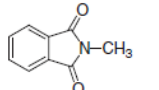
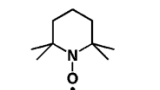
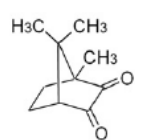
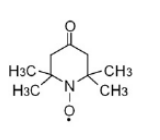
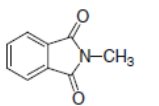
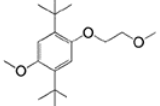
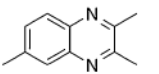
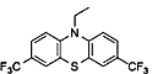
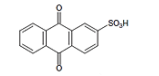
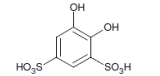
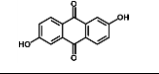
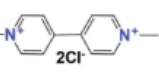
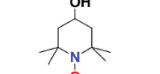
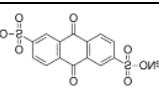
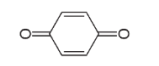
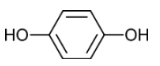
### **Electrochemical Characterization of Our Membrane-Free Battery.**

To obtain polarization curves, the Membrane-Free battery was first charged to the desired SOC (from 5% to 90%) and then polarized by point-by-point galvanostatic holds from 0 to 1 mAcm<sup>-2</sup>.

To conduct galvanostatic discharge experiments, the Membrane-Free battery was first galvanostatically charged to 35% SOC and subsequently discharged at different current densities (from -0.025 mAcm<sup>-2</sup> to -0.4 mAcm<sup>-2</sup>), with voltage limits of 0.3 and 2.0 V. The capacity obtained in each deep discharge step is represented over the maximum theoretical capacity ( $C_i$ ) of the cell at 35% SOC (this is the maximum mAh that can be extracted from the cell taking into account the concentration of converted active species at this SOC).

Galvanostatic charge-discharge cycling experiments were performed at  $\pm 0.05 \text{ mAcm}^{-2}$  with voltage limits of 0.3 and 2.0 V (deep discharge cycles) or fixing the charging and discharging times to 30 minutes each at  $\pm 0.2 \text{ mAcm}^{-2}$  (short charge-discharge cycles). The capacity retention was calculated by dividing the number of discharged coulombs during the  $n^{\text{th}}$  cycle by the discharged coulombs occurring during the first cycle. The energy efficiency (EE) was calculated as; coulombic efficiency (CE)  $\times$  voltage efficiency (VE).

Table S1. Comparison of technical parameters and key factors of reported Organic-RFBs

	Anolyte	Catholyte	Separator	Media	V (V)	CE (%)	EE (%)	Cycles	C retention	P (W/cm <sup>2</sup> )	Highlights	Ref
Non-Aqueous Organic RFB	 2,3,6-trimethylquinoxaline	 DBBB	Nafion 117	LiBF <sub>4</sub> in PC	1.3	70	37	30	100 (non-Flow)	8·10 <sup>-5</sup>	Coin cell configuration. Low CE and EE	[10]
	 MPh	 TEMPO	Nepem 117	NaClO <sub>4</sub> in ACN	1.36	90	74	20	-	4.7·10 <sup>-4</sup>	First example of “all organic RFB”	[11]
	 Camphorquinone	 4-Oxo TEMPO	Fuma Tech	TEABF <sub>4</sub> in PC	2.03	80	71	3	(95) (non-Flow)	0.002	Novel organic molecules providing higher operating voltages. Only 3 cycles of charge-discharge.	[12]
	 MePh	 DBMMB	Daramic /Celgard	LiTFSI in DME	1.9	90	69	50	100	0.066	Using porous separators results in high current densities. Mixed reactant electrolytes are necessary to mitigate crossover.	[13]
	 TMeQ	 BCF3EPT	Nafion 117	LiBF <sub>4</sub> in PC	1.3	85	42	50	0 (non-Flow)	2·10 <sup>-4</sup>	Swagelok cell configuration. Huge capacity loss over time.	[14]
Aqueous Organic RFB	 AQS	 BQDS	Nafion 112	H <sub>2</sub> SO <sub>4</sub>	0.45	90	40	12	90	0.0036	First example of all-organic aqueous RFB.	[15]
	 2,6-DHAQ	[Fe(CN) <sub>6</sub> ] <sup>4-</sup> Ferrocyanide	Nafion 212	KOH	1.1	99	84	100	90	0.45	Alkaline Flow Battery	[16]
	 Methyl-Viologen	 4-OH-TEMPO	AEM	NaCl	1.05	100	72	100	99	0.042	Neutral pH. High OCV and current densities	[17]
	 AQDS	Br	Nafion 212	H <sub>2</sub> SO <sub>4</sub>	0.65	95	55	15	99.2	0.6	Increasing in the OCV about 11% by adding -OH groups in AQDS	[18]
	 pBQ	 H <sub>2</sub> Q	Membrane-Free	HCl/PYR <sub>14</sub> TFSI	0.9	100	70	75	100	6·10 <sup>-4</sup>	Proof-of-concept of Membrane-Free battery.	This Work

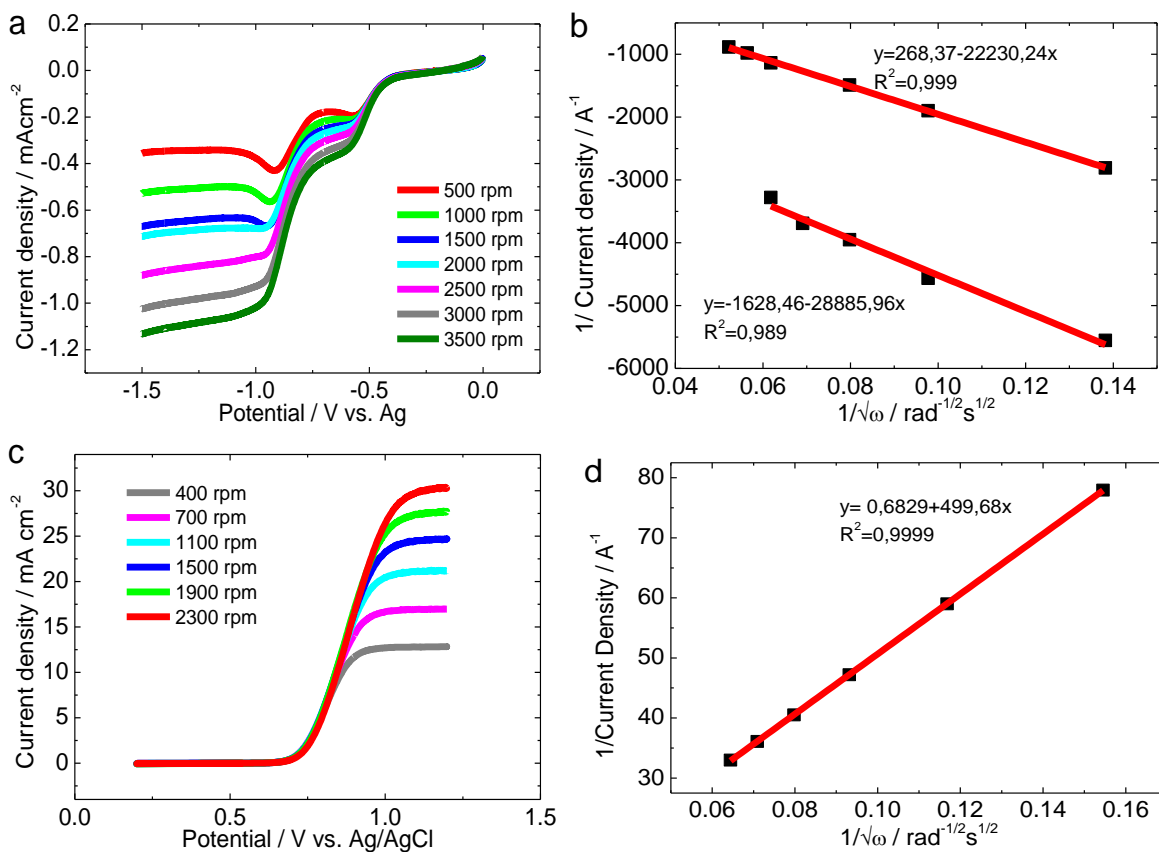


**Figure S1. Electrochemical investigation of redox electrolytes using a Rotating Disk Electrode (RDE).** **a**, RDE experiments (LSV at  $10 \text{ mVs}^{-1}$ ) of 5 mM pBQ in PYR<sub>14</sub>TFSI. **b**, Levich plot of 5 mM pBQ in PYR<sub>14</sub>TFSI and the line fit (red line) with its mathematical expression. **c**, RDE experiments (LSV at  $10 \text{ mVs}^{-1}$ ) of 20 mM H<sub>2</sub>Q in 0.1 M HCl. **d**, Levich plot of 20 mM H<sub>2</sub>Q in 0.1 M HCl.



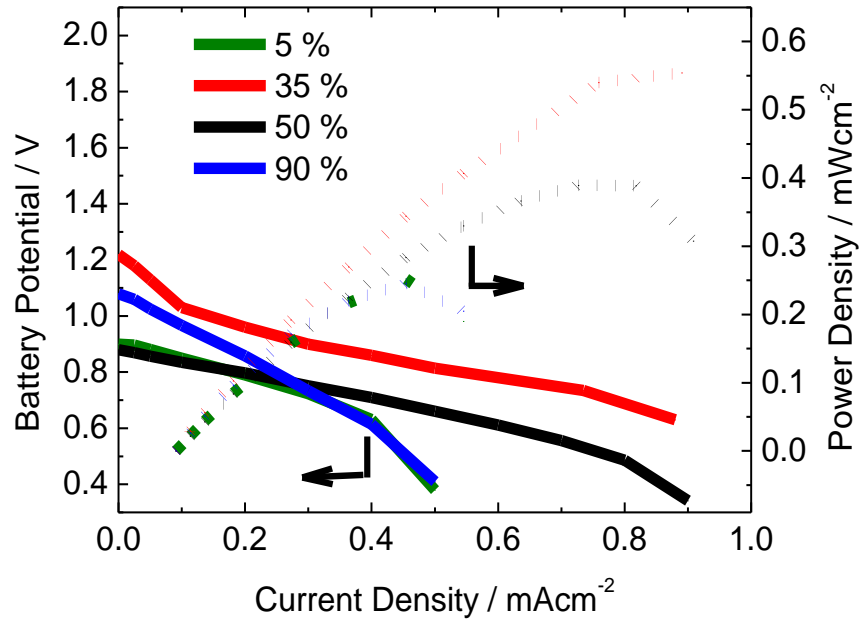


**Figure S2. Polarization curves of our Membrane-Free battery at four different states of charge (SOC).** All data were collected at room temperature using a 20 mM pBQ in PYR<sub>14</sub>TFSI solution as the anolyte and 20 mM H<sub>2</sub>Q in 0.1 M HCl as the catholyte.

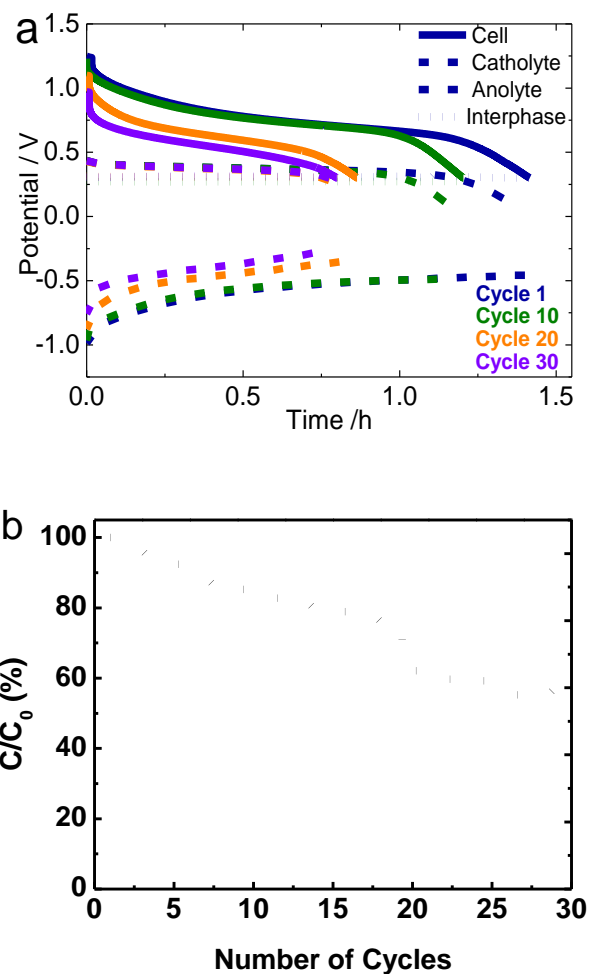


**Figure S3. Membrane-Free battery performance at 35 % SOC. Composition of the electrolytes: 20 mM pBQ in PYR<sub>14</sub>TFSI and 20 mM H<sub>2</sub>Q in 0.1 M HCl. (a) Cyclability test at  $\pm 0.05 \text{ mAcm}^{-2}$  using voltage cut-offs of 0.3 V in discharge and 2 V in charge (profound discharge). Discharge curves of 1<sup>st</sup>, 10<sup>th</sup>, 20<sup>th</sup> and 30<sup>th</sup> cycles with their individual profiles: Voltage of the full battery (continuous line), catholyte and anolyte individual voltages (dashed lines) and voltage drop at the interphase (dotted line); (b) Capacity retention vs. cycle number.**

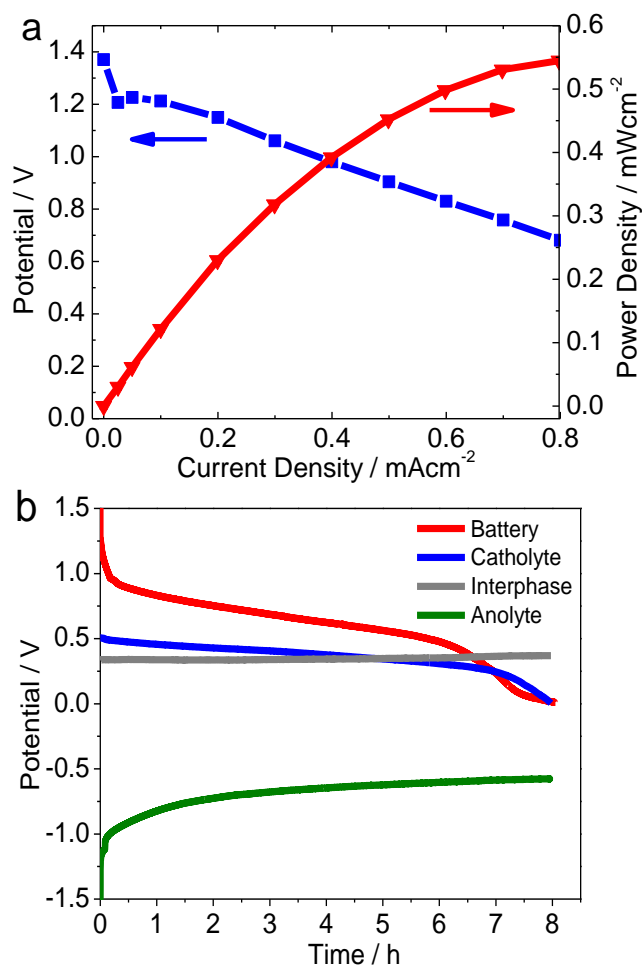


**Figure S4. Membrane-Free battery performance at 35% SOC. Composition of the electrolytes: 0.1 M pBQ in PYR<sub>14</sub>TFSI and 0.1 M H<sub>2</sub>Q in 0.1 M HCl.** (a) Cell potential and power density versus current density. (b) A galvanostatic charge-discharge cycle with the individual potential profiles at  $\pm 0.05$  mAcm<sup>-2</sup>.

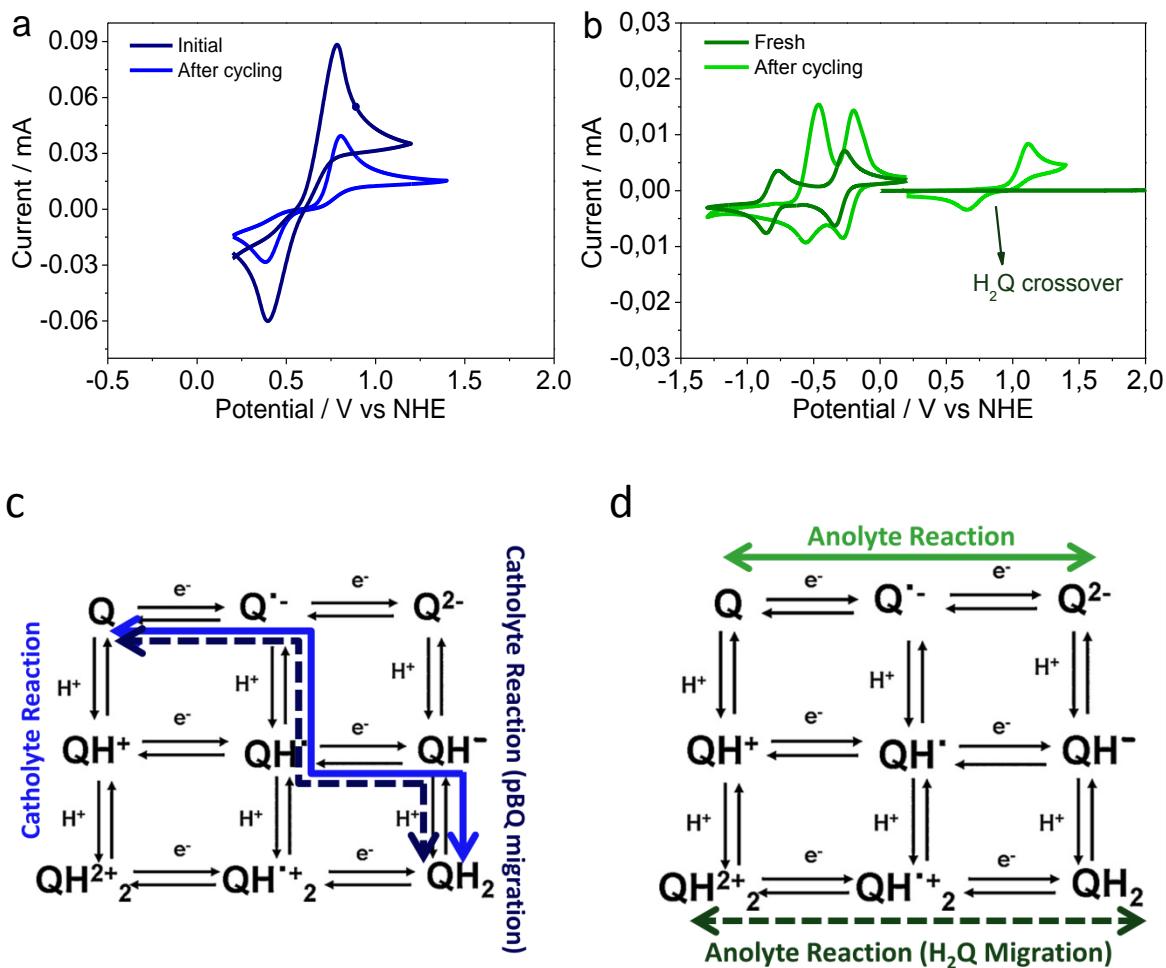


**Figure S5. Electrochemical investigation of the two immiscible electrolytes before and after cycling. Electrolyte active species concentration: 10 mM.** (a) CVs of catholyte. (b) CVs of anolyte. (c) Reaction mechanism and pathways for catholyte: Dissolved species (continuous line) and species coming from anolyte (dotted line). (d) Reaction mechanism and pathways for anolyte: Dissolved species (continuous line) and species coming from catholyte (dotted line).

## References

- [1] B. Huskinson, M. P. Marshak, C. Suh, S. Er, M. R. Gerhardt, C. J. Galvin, X. Chen, A. Aspuru-Guzik, R. G. Gordon, M. J. Aziz, *Nature* **2014**, *505*, 195–8.
- [2] R. Salazar, J. Vidal, M. Martínez-Cifuentes, R. Araya-Maturana, O. Ramírez-Rodríguez, *New J. Chem.* **2015**, *39*, 1237–1246.
- [3] X. Ji, C. E. Banks, D. S. Silvester, A. J. Wain, R. G. Compton, *J. Phys. Chem. C* **2007**, *111*, 1496–1504.
- [4] W. Sun, Q. Jiang, M. Yang, K. Jiao, *Bull. Korean Chem. Soc.* **2008**, *29*, 915–920.
- [5] Y. She, Y. Tang, H. Liu, P. He, *Chem. Cent. J.* **2010**, *4*, 17.
- [6] E. Laviron, *J. Electroanal. Chem. Interfacial Electrochem.* **1984**, *164*, 213–227.
- [7] C. Rüssel, W. Jaenicke, *J. Electroanal. Chem.* **1984**, *180*, 205–217.
- [8] T. Nagaoka, S. Okazaki, *J. Phys. Chem.* **1985**, *89*, 2340–2344.
- [9] M. A. Bhat, *Electrochim. Acta* **2012**, *81*, 275–282.
- [10] F. R. Brushett, J. T. Vaughey, A. N. Jansen, *Adv. Energy Mater.* **2012**, *2*, 1390–1396.
- [11] Z. Li, S. Li, S. Liu, K. Huang, D. Fang, F. Wang, S. Peng, *Electrochem. Solid-State Lett.* **2011**, *14*, A171–A173.
- [12] S. K. Park, J. Shim, J. Yang, K. H. Shin, C. S. Jin, B. S. Lee, Y. S. Lee, J. D. Jeon, *Electrochem. commun.* **2015**, *59*, 68–71.
- [13] X. Wei, W. Duan, J. Huang, L. Zhang, B. Li, D. Reed, W. Xu, V. Sprenkle, W. Wang, *ACS Energy Lett.* **2016**, 705–711.
- [14] A. P. Kaur, N. E. Holubowitch, S. Ergun, C. F. Elliott, S. A. Odom, *Energy Technol.* **2015**, *3*, 476–480.
- [15] B. Yang, L. Hooper-Burkhardt, F. Wang, G. K. Surya Prakash, S. R. Narayanan, *J. Electrochem. Soc.* **2014**, *161*, A1371–A1380.
- [16] K. Lin, Q. Chen, M. R. Gerhardt, L. Tong, S. B. Kim, L. Eisenach, A. W. Valle, D. Hardee, R. G. Gordon, M. J. Aziz, et al., *Science (80-. )*. **2015**, *349*, 1529–1532.
- [17] T. Liu, X. Wei, Z. Nie, V. Sprenkle, W. Wang, *Adv. Energy Mater.* **2016**, *6*, DOI 10.1002/aenm.201501449.
- [18] B. Huskinson, M. P. Marshak, C. Suh, S. Er, M. R. Gerhardt, C. J. Galvin, X. Chen, A. Aspuru-Guzik, R. G. Gordon, M. J. Aziz, *Nature* **2014**, *505*, 195–198.